

# Locating Liquid-Liquid Interfaces Using an Underwater Buoyancy-Regulating Robot, Altering Volume with Embedded Electromechanical Actuation

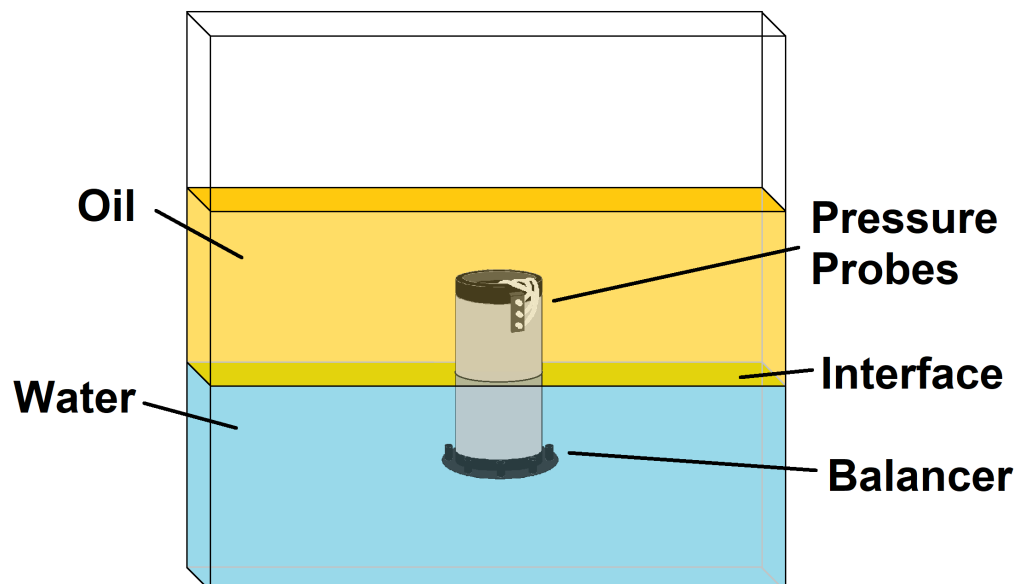
Julian Brandt - jubr@itu.dk

Mads Ørnfeldt Wolff Jespersen - oeje@itu.dk

Nicolai Pallund - npal@itu.dk

June 2023

KISPECI1SE



# Contents

<b>1 Abstract</b>	<b>4</b>
<b>2 Introduction</b>	<b>5</b>
<b>3 Background</b>	<b>6</b>
3.1 Locating Interfaces Between Liquids . . . . .	6
3.2 Contemporary Buoyancy Control in Underwater Robots . . . . .	7
3.2.1 Underwater Buoyancy Regulating Bladder Robot . . . . .	7
3.2.2 Underwater Flexible Fish Robot . . . . .	7
3.2.3 Ocean Surveying M-AUE . . . . .	8
<b>4 Methodology</b>	<b>8</b>
4.1 Key Issues . . . . .	8
4.1.1 Determining Depth of Robot . . . . .	8
4.1.2 Determining Density of Liquids . . . . .	9
4.1.3 Achieving Sufficient Expansion and Precision of Movement . . . . .	10
4.2 Prototype and Experiments . . . . .	10
4.2.1 Prototype overview . . . . .	10
4.2.2 Density Estimation in Multi-phase Liquids . . . . .	11
4.2.3 Depth Estimation from Density . . . . .	12
4.2.4 Impact of Robot Angle on Differential Pressure Sensor . . . . .	12
4.2.5 Relationship between Internal Air Pressure and Total Expansion .	13
<b>5 Results</b>	<b>13</b>
5.1 Density Estimation in Multi-phase Liquids . . . . .	13
5.2 Depth Measuring . . . . .	15
5.2.1 Measuring depth from pressure . . . . .	15
5.3 Impact of Robot Angle on Differential Pressure Sensor . . . . .	16
5.4 Relationship between Internal Air Pressure and Total Expansion . . . . .	17
5.5 Additional Findings in Buoyancy Control . . . . .	18
5.5.1 Calculated Density As Measurement Of Buoyancy . . . . .	18
5.5.2 Momentum Creating Bobbing Motion . . . . .	19
<b>6 Discussion</b>	<b>20</b>
6.1 Weight Balancing to Reduce Tilt . . . . .	20
6.2 Tilt Compensation . . . . .	20
6.3 Measuring Depth with IMU VS Absolute Pressure Sensor . . . . .	21
6.4 Buoyancy Control . . . . .	22
6.4.1 Alternative Method of Monitoring Robot Expansion . . . . .	22
6.4.2 Cavities In Robot Housing Trapping Liquids Through Phases .	22
6.4.3 Overcoming Expansion Force Limitations . . . . .	22
6.5 Further Work . . . . .	23
6.5.1 Mapping a Column of Multiple Liquids . . . . .	23
6.5.2 Characterizing Emulsion In Liquids . . . . .	25
6.5.3 Alternative Methods of Volume Change . . . . .	25
<b>7 Conclusion</b>	<b>26</b>
<b>8 References</b>	<b>27</b>

<b>Appendices</b>	<b>29</b>
<b>A Prototype model and dimensions</b>	<b>29</b>
<b>B Prototype Technical Drawing</b>	<b>30</b>
<b>C Prototype Wiring Diagram</b>	<b>31</b>
<b>D Photograph of Prototype in Oil/Water Interface</b>	<b>32</b>
<b>E Relevant 3D Printed Parts</b>	<b>33</b>

# 1 Abstract

Locating liquid-liquid interfaces is an important task in many fields of industry. In this paper, our aim is to address the problem using robotics, by developing a buoyancy-regulating robot to find the depth of interfaces between water and sunflower oil. As a part of our approach, we summarize relevant advancements in buoyancy-regulating robotics, which influenced the creation of our prototype for the task.

The prototype utilizes electromechanical actuation as means of changing its volume, enabling it to sink or float in different fluids. It is constructed inside a waterproof cylindrical housing, and measures external liquid pressure via rubber tubes, thereby facilitating the calculation of liquid density and depth.

Using the prototype, we have gathered data to assess its accuracy and precision in locating liquid densities and depths, as well as to identify the requirements and constraints necessary for constructing robots in this domain.

The prototype can increase its volume by 12.6%, and, in experiments, calculate the depth of an oil/water interface with an error of  $0.73\text{cm}$  or 6.8%. Additionally, the prototype can calculate the densities of water and oil with a relative error of  $\pm 1.4\%$ .

We discovered issues relating to the robot's shape trapping liquids, overcoming counteracting forces on actuator, sensor drift, and tilt lowering the ability to measure density through differential pressure. We discuss and suggest possible solutions to these problems.

Finally, we propose avenues for further work, which include characterizing emulsified interfaces and exploring alternative methods of volume change. Additionally, we have devised an algorithm for identifying multiple interfaces within a column of liquid, however it was not implemented during this project.

## 2 Introduction

In various industries and scientific fields, the separation of liquids with multiple phases is an important task. This often requires finding the depth of the interface between these liquids, which can be difficult and sometimes requires specialized equipment [2, 5]. By creating an all-in-one robot-solution to the interface finding problem, the process could potentially be generalized and require less specialized equipment in different use cases, lowering operation costs in their respective fields. This paper documents our prototype of a buoyancy-regulating robot to solve the problem of locating liquid interfaces. More specifically, we aim to answer the following:

**How can a buoyancy-manipulating robot, using electromechanical actuators, be designed to approximate the location of an interface between water and oil, and what are the requirements and constraints for a prototype of such a robot to maximize its precision and accuracy in locating interfaces?**

This question can be seen as twofold: achieving autonomous buoyancy control using electromechanical actuators, and locating the interface between liquids. Each of these questions can be expanded respectively to: **How can the precision of buoyancy control be maximized, such that it is predictable and repeatable, and provides the most sophisticated motion control for finding liquid interfaces?**, and **How can the depth of a robot best be approximated in liquids with multiple phases?**

We have observed a lack of utilization of electromechanical actuators in current buoyancy-regulating robots. We have identified what we believe to be inherent advantages associated with these actuators when effectively implemented, including a high potential volume range and high actuation speed [14].

In order to effectively address the research questions, we have intentionally chosen to exclude the analysis of certain phenomena in liquids such as waves, turbulence and friction, as well as simplifying applied pressures and forces. This decision was made to streamline our research and allow us to concentrate on the specific objectives related to buoyancy control and interface detection in immiscible liquids as put forth by our research questions. By limiting the scope in this way, we aim to achieve a more comprehensive understanding of the challenges within the specific research domain.

### 3 Background

#### 3.1 Locating Interfaces Between Liquids

Locating interfaces in multi-phase fluids is a field with much interest in new technology [13, 15]. Detecting where immiscible liquids separate is a necessary task in chemistry processes as well as crude oil extraction where it lets you extract the correct amount of liquid [5, 2].

Due to the widespread relevance of interface locating solutions, numerous approaches have been developed to address this task effectively. The paper *Interface Layers Detection in Oil Field Tanks: A Critical Review* [5] describes many currently applied methods of locating the interface between water and crude oil, in the process of extracting crude oil.

By exploring and understanding these existing methods, it becomes possible to enhance and further contribute to the advancements in detecting and locating interfaces in multi-phase liquids. The paper mentions the following methods:

- **Differential liquid pressure** - A vertical array of pressure sensors measuring pressure at different depths to detect where the density changes. By detecting density changes, the interface between liquids can be located.
- **Capacitive sensing** - Measuring conductivity of liquid between two plates on a probe. By detecting changes in conductivity, the interface can be located.
- **Microwaves** - Measuring travel time of the echoes can tell the depth of the interfaces.
- **Radiation** - Radioisotopes, such as gamma sources, are lowered into the liquid along with a collector, and the amount of observed radiation can be used to determine which liquid the sensor is in. When the amount absorbed by the liquid changes, the sensor must be at the interface.
- **Displacers / Floats** - Multiple floats are deployed with specific densities matching specific interfaces.
- **Vibrating switches** - measuring dampening of an output frequency. Various liquids exhibit varying degrees of dampening, allowing for interface detection.
- **Optical fiber** - Measuring pressure and temperature of liquid. The cladding of the optical fiber is removed at a certain interval, and the light is exposed to the liquid. The refractive index of the liquid determines how much power is drained out of the fiber.
- **Ultrasound** - Utilizing the differences in acoustic properties in different liquids to locate the interface.

The majority of these solutions, while novel and advantageous in their own right, are not well-suited for implementation on an autonomous robot which operates within the liquid itself. This constraint particularly affects methods reliant on the time of flight (TOF) of a signal, as they often require a fixed orientation and position to accurately send and receive the signal they emit. Most of these methods circumvent this by having the emitter and sensors as a part of the container that holds the liquid.

The paper also describes that several of these methods are impacted by direct contact with the liquids, as it can cause issues with corrosion on the materials or cause buildup on the sensors [5, p. 183]. This can significantly reduce the lifespan of components without regular maintenance.

It is also important to consider the choice of materials for the solution. For example, natural rubber is weakened in oil, which is why it is important to pick materials which comply to the specific constraints set forth by the liquids [1]. This project will not put too much focus on the choice of materials, but we acknowledge that it is an important part of building a robot for the use case.

In industrial processes, liquids often contain contaminants and varying quantities of dissolved materials, leading to changes in liquid properties and the formation of emulsion layers between different liquid phases. Emulsion layers create challenges for many existing methods, as the emulsion blurs the line between the phases [5, p. 181-190].

Additionally, some methods rely on knowing the densities of liquids beforehand for accurate depth calculations, therefore it might be advantageous to instead measure the density in real time when applying these methods when contaminants are present.

Among the various methods explored, one approach that shows promise for an autonomous robot is the utilization of differential pressure across a known difference in depth, to measure liquid density. This is because pressure is a very direct measurement of the liquid. It works well, as the environment, such as liquid container shape, has little to no effect on readings, which cannot be said for TOF-reliant methods.

## 3.2 Contemporary Buoyancy Control in Underwater Robots

In the domain of underwater robotics, there exists many different underwater robot designs that utilize buoyancy control as part of their movement. In this section we discuss three relevant implementations, which showcase different methods for regulating buoyancy.

### 3.2.1 Underwater Buoyancy Regulating Bladder Robot

In the paper *Electromechanical Control and Stability Analysis of a Soft Swim-Bladder Robot Driven by Dielectric Elastomer*, a buoyancy control system is implemented with the use of a dielectric elastomer actuator (DEA), which strains when high voltage runs through it [10]. This implementation also utilizes a ring of variable ballast to balance the prototype, in the case that the robot is naturally off balance.

Using a DEA to achieve variable buoyancy can be quite precise, but outside pressure poses a challenge as outside pressure will counteract the expansion force of the DEA. Another consideration is that the high voltages used might not be desirable for some use cases, and can be difficult to generate and manage.

### 3.2.2 Underwater Flexible Fish Robot

A robotic fish with two precise piston-like internal buoyancy units, that mimic a real fish, is described in the paper *Exploration of underwater life with an acoustically controlled soft robotic fish* [12]. The two buoyancy units act as internal bladders that can change their volume to change the robot's buoyancy to aid in underwater movement, and be driven independently to control the pitch of the robot.

### 3.2.3 Ocean Surveying M-AUE

In the paper *A swarm of autonomous miniature underwater robot drifters for exploring submersible ocean dynamics* [9], a so called *M-AUE* underwater robot uses two syntactic foam cylinders which forms an inner and outer shell. These two parts are connected through a piston, which pushes the two pieces apart to increase or decrease the robot's volume. This approach of utilizing an electromechanical actuator enables direct control of buoyancy and opens up the possibility of using off the shelf components, as opposed to more exotic ways of achieving buoyancy control.

## 4 Methodology

There are many methods to detect and locate interfaces, such as utilizing ultrasonic, optical or pressure sensors. However, each solution also has its own set of issues, depending on the characteristics of the liquids. As explained in section 3.1, there are fewer environmental constraints when using pressure sensors as means of depth measurement, which is why this method is chosen for constructing a prototype of an interface-locating robot.

### 4.1 Key Issues

To achieve the goals set forth in the research questions, noted in section 2, and create an all-in-one robotic solution for the task, we have identified the following distinct problems that need to be overcome in order to successfully identify the depth of interface(s) between immiscible liquids: determining the current depth of a submersed robot, dynamically determining the density of a liquid, and achieving sufficient expansion and precision of movement.

#### 4.1.1 Determining Depth of Robot

It is possible to calculate the depth of the robot in a liquid if given the pressure, due to the linear relationship between depth and hydrostatic pressure. For example, for every meter of depth in room temperature water, pressure increases by approximately 100 hPa. Hydrostatic pressure is the pressure created by the weight of the column of liquid above a given area. The hydrostatic pressure can be calculated with a formulation of Bernoulli's equation:

$$p = \rho \cdot g \cdot h$$

The three terms are the density of the liquid  $\rho$ , the gravitational constant  $g$ , and the height of the column of liquid above the object  $h$  [3, p. 125]. This formulation does not take phenomena such as compression of liquid or turbulence into account.

When the density and pressure of the liquid is known, this formulation can be solved for  $h$  to find the depth.

However, when additional phases of liquid are introduced, more complex calculations are required. Each phase contributes its own hydrostatic pressure, resulting in a non-linear correlation between pressure and depth. Instead, there are distinct steps in the relationships. For example, as shown in Figure 1, when comparing 1 meter of vegetable oil and 1 meter of water to 2 meters of water, the combined hydrostatic pressure would be approximately +190hPa for the mixture and +200hPa for pure water. This is because the density of vegetable oil is approximately 90% of the density of water.

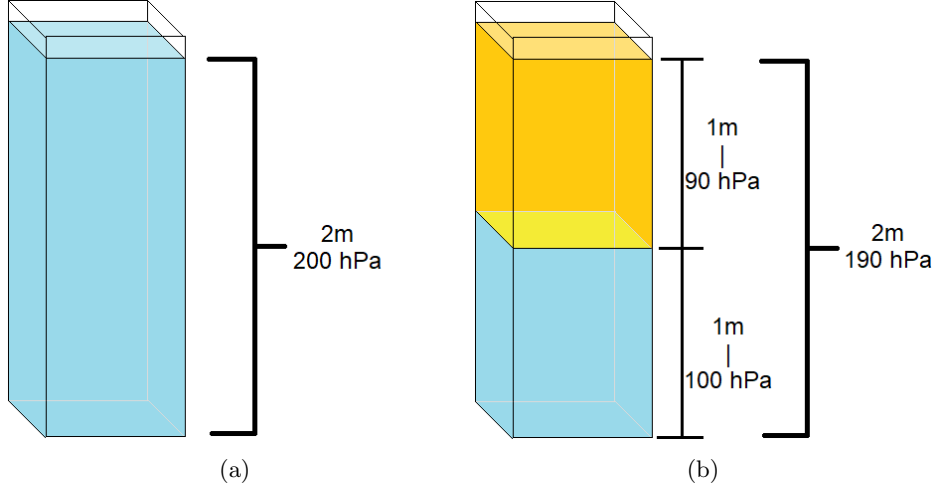


Figure 1: Diagram of phases contributing different hydrostatic pressure based on liquid density

#### 4.1.2 Determining Density of Liquids

To ensure accurate finding of interfaces through liquid pressure, it is necessary to determine the density of all liquids above the interface. Knowing the density of the liquids is crucial due to liquid pressure being proportional to density, allowing for dynamic determination of depth at a given interface.

It is possible to determine the density of a liquid by measuring the difference in hydrostatic pressure between two points of depth. Hydrostatic pressure increases linearly with increasing depth. The rate at which pressure increases with depth is determined by the density of the liquid.

Bernoulli's equation can be rearranged to calculate the density of a liquid given a delta of pressure and depth:

$$d = (\Delta p) / (g \cdot (\Delta h))$$

Here,  $\Delta p$  is the change in pressure and  $\Delta h$  is the change in depth.

Consider an example where pressure readings are taken at two different points in a liquid, with a difference in depth of 10 cm. The pressure values are measured as 102,305Pa and 103,285Pa respectively. By applying these values to the equation, we can calculate the density of the liquid.

$$d = \frac{103285Pa - 102305Pa}{9.81m/s^2 \cdot 0.1m} = 998.98kg/m^3$$

The calculated density of the liquid is approximately 998.98kg/m<sup>3</sup>. This value is roughly the density of water at 25 degrees Celsius.

### 4.1.3 Achieving Sufficient Expansion and Precision of Movement

Movement can be achieved by physical expansion of the robot's volume. This is because buoyancy of an object is tied to its density. If the mass of the robot remains the same, but the volume is variable, then the density is variable, and therefore the buoyancy is variable.

The buoyancy of an object is the combined effect of two forces: the buoyant force and gravitational force, and is what determines if an object sinks, floats or is neutrally buoyant.

To calculate the buoyancy of an object, we use a formulation of Archimedes' principle combined with Newton's second law of motion([3, pp. 42, 96]).

$$F = -\rho \cdot g \cdot V + m \cdot g$$

Where  $\rho$  is the density of the liquid,  $m$  is the mass of the object,  $g$  is the gravitational constant and  $V$  is the volume of the object.

To locate interfaces in liquids of different densities, the robot will have to be able to set its own density to match these liquids. The difference between the maximum and minimum required density of the robot we define as its buoyancy range. Ideally, the robot would be capable of functioning in any density. However, in reality, a volume-changing robot can only adjust its volume within a certain range. Therefore, it is important to optimize the mass and volume range to accommodate the specific densities that the robot should be able to navigate.

In addition to the total achievable change in buoyancy, the robot might also need a finer resolution of expansion for liquids whose densities are very close to each other.

## 4.2 Prototype and Experiments

In order to understand and come up with solutions to the identified key issues, we designed and constructed a prototype of an interface-locating robot. The prototype robot consists of three primary embedded systems: an expansion mechanism, a density sensing system, and a depth sensing system. First, an overview of the prototype will be given, and then each major part of the robot will be described in more detail when they become relevant. Afterwards we describe experiments involving the built prototype, which will help find solutions to the key issues outlined in section 4.1.

### 4.2.1 Prototype overview

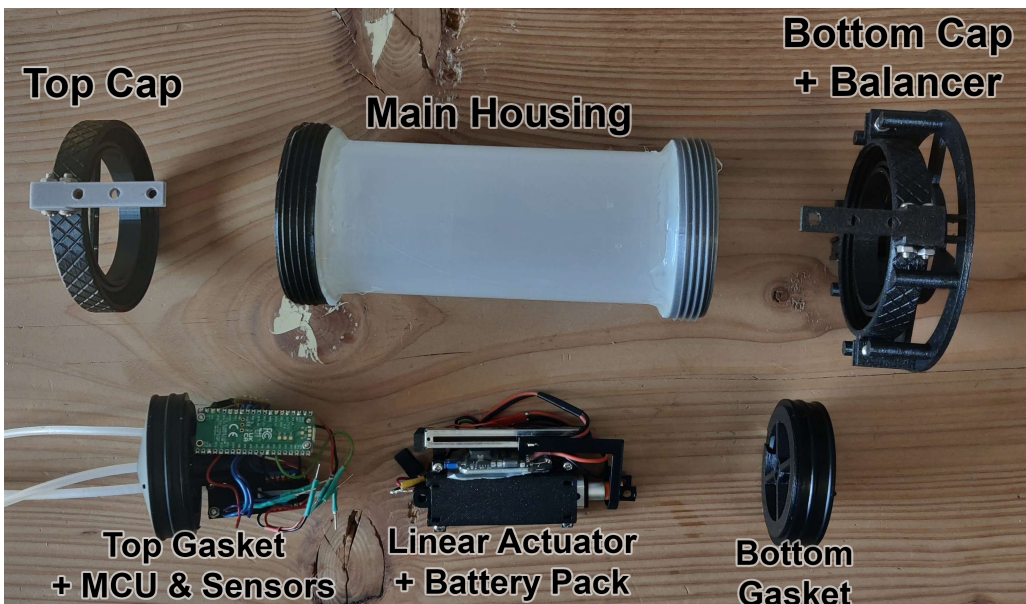
The robot's housing is built using a modified dosing syringe. The ends of the syringe are removed, with waterproofing ensured by movable rubber gaskets in each end. The housing also features two end-stops to prevent the gaskets from protruding beyond the housing body. The fully assembled robot can be seen in Figure 2a

The internal electronics consists of a Raspberry Pi Pico W, a 6V 128N linear actuator, which can extend up to three centimeters, an inertial measurement unit (IMU), two absolute pressure sensors; one for measuring internal pressure and one for external pressure, a differential pressure sensor, a linear potentiometer on the actuator, as well as batteries and voltage regulators to power the system.

This makes up a watertight robot taking up 808 ml and weighing a minimum of 528 g. It can increase its total volume by up to 102.64 ml, and therefore manipulate its own density to a minimum of 0.5798 kg/L and variable maximums based on additional ballast. The robot captures various relevant pressure and movement data, and remain completely wireless, as data is transmitted over wireless communication. A breakdown of the construction can be seen in Figure 2b.



(a) Assembled view of the robot.



(b) Exploded view of the robot housing and the internals.

Figure 2: Assembled and exploded views of the complete prototype

#### 4.2.2 Density Estimation in Multi-phase Liquids

Instead of measuring densities manually and feeding the values to the robot, having onboard instruments to measure density makes the robot fully autonomous. We have chosen to use a differential pressure sensor for this purpose. We use the sensor to capture a pressure delta over a known depth range, and then calculate the density from the read pressure, as pressure and density is directly correlated due to hydrostatic pressure being linear in depth, as established in 4.1.2.

Rubber tubes run from the differential pressure sensor to the outside where they are mounted onto the top cap with a known distance of 3cm between them. The hollow rubber tubes allow external pressure to compress the air inside them, while letting the sensor sit inside the main housing.

This method of measuring density relies on the assumption that the depth difference between the tubes corresponds precisely to the known distance of 3cm. To ensure the robot maintains the necessary orientation for accurate measurements, it is designed to remain upright during operation, aided by a balancer ring at the bottom. This balancer ring allows for the attachment of adjustable ballast, facilitating optimal alignment with the sensor for reliable density calculations.

To determine how reliable the robot is at finding liquid density and distinguishing between liquids, we will conduct an experiment, where we move probes of the differential pressure sensor between water and oil. By doing this, we can compare the measured densities with the actual densities, allowing us to evaluate the accuracy of the measurements.

#### 4.2.3 Depth Estimation from Density

To estimate the depth, the robot employs both the external pressure and density measurement, utilizing the formula for hydrostatic pressure as stated in 4.1.1. An absolute pressure sensor is used to measure the external pressure. A rubber tube extends from the sensor to the outside liquid and is mounted onto the top cap, between the tubes from the differential pressure sensor.

Because hydrostatic pressure is only linear per phase, when dealing with multiple liquid phases, the prototype needs reference points to the surface of each phase. When an interface is found, it is used as a reference point until a potential next interface is found. This lets the robot isolate the pressure exerted by each phase, making multi-phase depth estimation possible.

In practice, this would work by slowly lowering the buoyancy of the robot so the robot can settle on each different layer. The pressure at the interface could then be logged, creating a map of known densities and the respective pressure values.

To measure the prototype's ability to estimate depth, we will conduct experiments letting the robot float and sink in a liquid column continuously. This will be done in water alone, and a mixture of water and oil. We will then determine the robot's precision in providing consistent pressure readings, and the accuracy of the readings compared to the actual depth.

#### 4.2.4 Impact of Robot Angle on Differential Pressure Sensor

The differential pressure sensor is used to provide the difference in pressure between the two onboard probes, which are routed to the outside with rubber tubes. As the sensor can only capture the depth difference between the probes, the placement of the tubes are essential to a useful reading.

In the prototype, the probes of the sensor are fixed 3 cm vertically above one another, but during operation, tilt on the robot would make the vertical distance shorter. A shorter vertical distance means less of a difference in pressure, which makes readings incorrect, if we assume the same depth difference of 3 cm at all times.

In order to explore the impact of different angles of tilt, we conduct an experiment, where we fix the probes 3 cm apart in a rotating brace underwater and lowering the vertical distance between them by rotating the brace 5 degrees at a time. In theory, the measured pressure should follow a sine curve as the brace rotates, because the probes are rotated in a circle. The rotating jig can be seen in Appendix E.

#### 4.2.5 Relationship between Internal Air Pressure and Total Expansion

In order to correctly identify the robot's current density, and therefore its current buoyancy, it is crucial to know the amount of expansion at any given time.

In the prototype, the expansion mechanism works by a linear actuator that pushes two movable rubber gaskets apart inside the housing by up to three centimeters. These gaskets are attached at each end of the linear actuator. Although only one movable gasket is required in principle, both gaskets can move independently due to assembly constraints. Since the gaskets can move independently of the robot housing, end-caps are included to prevent them from sliding out of the housing.

To determine the robot's degree of expansion, we use a linear potentiometer on the expansion mechanism to gauge how extended the linear actuator is.

However, as the robot is watertight, it should theoretically be possible to use the internal pressure as a measurement of expansion, as the air pressure inside drops as the mechanism expands. This change in pressure is due to the fact that the same mass of air is compressed or expanded to different volumes. The changes in volume can be calculated using Boyle's Law [3, p. 85]

$$P_1 \cdot V_1 = P_2 \cdot V_2$$

In this formulation,  $P_1$  and  $V_1$  are the pressure and volume before the change and  $P_2$  and  $V_2$  are the pressure and volume after the change. This means that if we know the initial pressure and volume ( $\mathbf{P}_1$  and  $\mathbf{V}_1$ ) and measure the pressure after a change in volume ( $\mathbf{P}_2$ ), we can calculate the new volume.

Comparing the data acquired from the linear potentiometer and the internal pressure sensor will verify if there is a relationship as expected, or show if there are any issues with the approach. The redundancy from having two different sensors could also provide the robot with a way of detecting leaks, by looking if there are discrepancies between the two measurements.

## 5 Results

### 5.1 Density Estimation in Multi-phase Liquids

Even though the density of liquid can theoretically be measured by a pressure difference between two points, we want to measure how effectively the robot can use this information to distinguish between liquids and find interfaces.

By repeatedly moving the differential pressure probes through an interface between water and sunflower oil, we have investigated how precisely and accurately the differential pressure sensor measures the density of each phase. The testing setup uses a brace to keep the tubes vertically separated by 3 cm. This means the expected differential pressure readings are 271 Pa for oil and 294 Pa for water, because sunflower oil's density is approximately 92% that of water [4]. These numbers are calculated based on the gravitational constant in Denmark of  $9.816m/s^2$ , which can vary at different places on Earth.

Calculating mean and standard deviations of measurements, the sensor quite accurately determines the density of water and oil, but has a higher standard deviation in water, which equates to lower precision. The values of mean and standard deviation can be seen in table 1. The expected measured density is around  $0.92\text{kg/L}$  for oil and  $1\text{kg/L}$  for water.

	Measured density of oil	Measured density of water
Mean $\mu$	$0.9073 \text{ kg/L}$	$1.014 \text{ kg/L}$
SD $\sigma$	$0.00597 \text{ kg/L}$	$0.01251 \text{ kg/L}$

Table 1: Table showing mean and standard deviation for density measured by differential pressure sensor.

Figure 3a is an excerpt of the data from measuring differential pressure in water and oil.

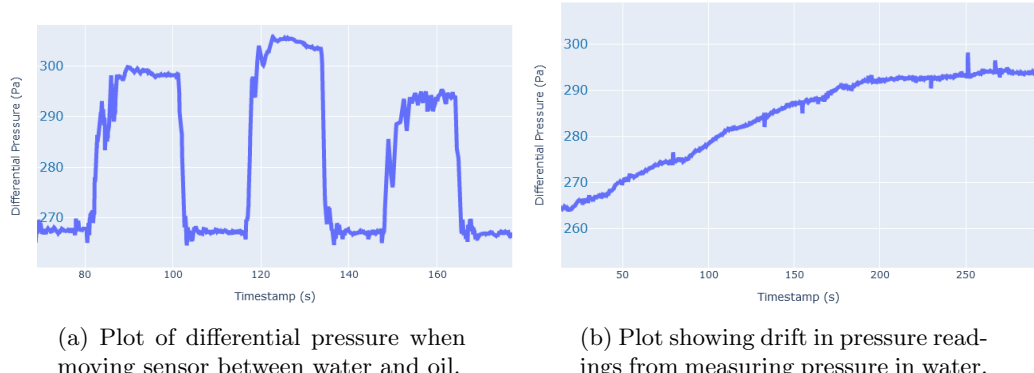


Figure 3: Plots of differential pressure measured by placing probes in liquid 3 cm apart

While it is clear from looking at Figure 3a, when the sensor measures water or oil, only the readings from oil are precise to the point we expected.

When the sensor is placed in oil, which are the low values in the graph, the measurement is  $267 \pm 1\text{Pa}$ . The  $4\text{ Pa}$  discrepancy, between the expected value and measured value, amounts to  $0.43\text{ mm}$  of depth. The discrepancy might thus be explained by the fact that the brace used for the testing setup was 3d-printed, and has error margins in this order of magnitude. When the sensor moves through the interface, into the water, which are the high values in the graph, the readings become somewhat irregular. This is visible in Table 1, where measurements in water have more than double the standard deviation of those in oil, although the mean of all water measurements are close to the correct value.

Examining the irregularities with water further, we conducted a separate experiment, moving the sensor between air and water, letting the readings settle. There is a noticeable drift from the initial values in water to when it levels out at the correct value. This can be seen in Figure 3b, where the pressure in water takes roughly 5 minutes to level out close to  $294\text{ Pa}$ , which is the expected pressure reading. We acknowledge that this drift can cause issues for density measurement, and that to get more accurate measurements we have to average readings over a period of time.

## 5.2 Depth Measuring

Seeing depth as a function of liquid pressure, we have simplified the depth estimation to pressure estimation. Measuring depth was done in water, which has a known density of nearly 1 kg/L. Data was taken for 50 continuous flow and sink movements, measuring the peaks of each motion to check whether the robot would report the same pressure after each repeated motion.

	Min pressure	Max pressure
Mean $\mu$	1019.21 hPa	1034.32 hPa
SD $\sigma$	0.1323 hPa	0.2417 hPa

Table 2: Table showing mean and standard deviation for pressure readings by robot at top and bottom of testing-aquarium during repeatability test. The mean values are relative to the experiment, because atmospheric pressure varies daily, and directly affects absolute readings from the robot.

The precision of the sensor allows us to get fairly stable readings of the surface and bottom of the liquid, with a standard deviation of  $0.1323\text{hPa}$  on the surface and  $0.2417$  at the bottom, as shown in Table 2. These standard deviations translate to  $\approx 1.32\text{mm}$  and  $\approx 2.42\text{mm}$ , since 1 cm of depth roughly translates to 1 hPa. There is a discrepancy between the standard deviations, which might be a result of the additional ballast attached to the bottom which can shift when the robot lands on top of it, but has no impact when the robot is floating at the surface. This can cause the readings at the bottom to be less consistent.

### 5.2.1 Measuring depth from pressure

Seeing as the measurements of pressure on the surface and at the bottom of the liquid are fairly repeatable, it is valuable to check whether these measurements are accurate in terms of the depth they represent.

In an experiment operating the robot in 39 cm of water, the robot determined the total depth to be between 37.2 and 37.92 cm. In another experiment, when trying to find an interface between water and oil at 10.7 cm below the surface, the robot determined the interface to be at 11.43 cm below the surface. While the surface and bottom readings in these experiments have low standard deviations, the composite result - the measured depth - diverges from the expected result more than expected. These depth measurements mean the robot calculated the depth of the interface to be 6.8% deeper than the actual location, and the total depth of the liquid to be between 3.8% and 4.6% less than the actual depth.

### 5.3 Impact of Robot Angle on Differential Pressure Sensor

To characterize the robot's ability to estimate density at an angle, we collected data from the differential pressure sensor when tilted at different angles.

Figure 4 shows the data points from fixing the probes 3 cm apart at different angles in water on a rotating jig. This is plotted against a prediction of what the readings should be at the given point. Numbers show the angle of the jig, 90 being horizontal, i.e. zero difference in pressure.

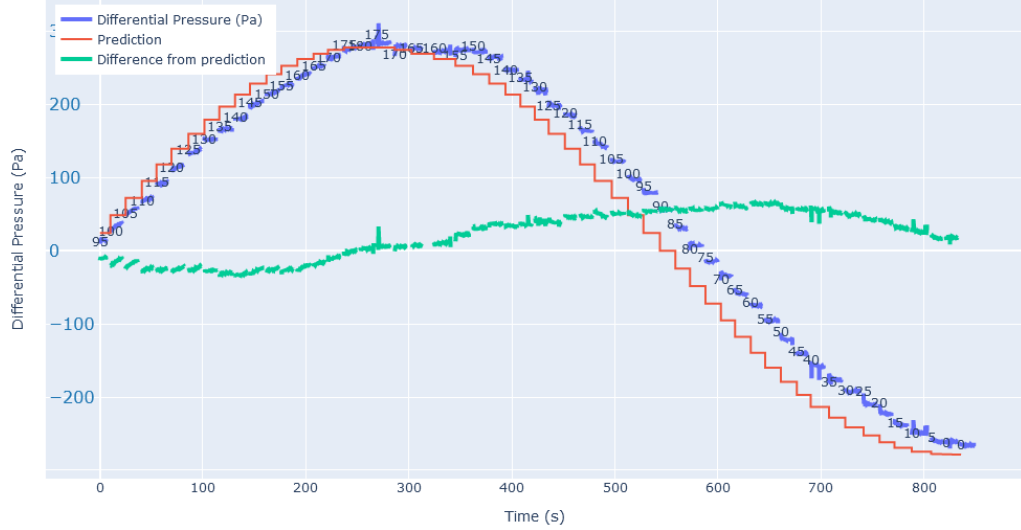


Figure 4: Plot of data from differential pressure experiment, where probing tubes are attached 3 cm apart on a rotating jig underwater.

By looking at the graph, the readings follow a sine curve, as expected when rotating the probes in a circle, albeit with a slight offset from the predicted values. This indicates that we can still calculate the correct density of the liquid when the angle changes, given that we can obtain the current angle of tilt.

The offset from the prediction line seems to be a result of the sensor used in the experiment, which in some cases needed extra time to stabilize on a value, which could create a lag in readings if not allowed to settle. In the experiment, the angle was changed every 10 seconds, so not much time was left to let the readings settle. Intermediate readings while rotating the jig have been left out of the graph.

Similar errors have been identified in the experiment described in 5.1, which might stem from the same issue. Interestingly, the offset also seems to follow a sine curve, which could indicate the offset can be predicted.

## 5.4 Relationship between Internal Air Pressure and Total Expansion

We have identified the internal air pressure of the robot as a potential key metric in buoyancy control, since it might replace the need for encoders or potentiometers on the expansion mechanism.

Collecting data from an internal pressure sensor and plotting it against the absolute expansion value gathered from the potentiometer, we can see a correlation, as shown in Figure 5a.

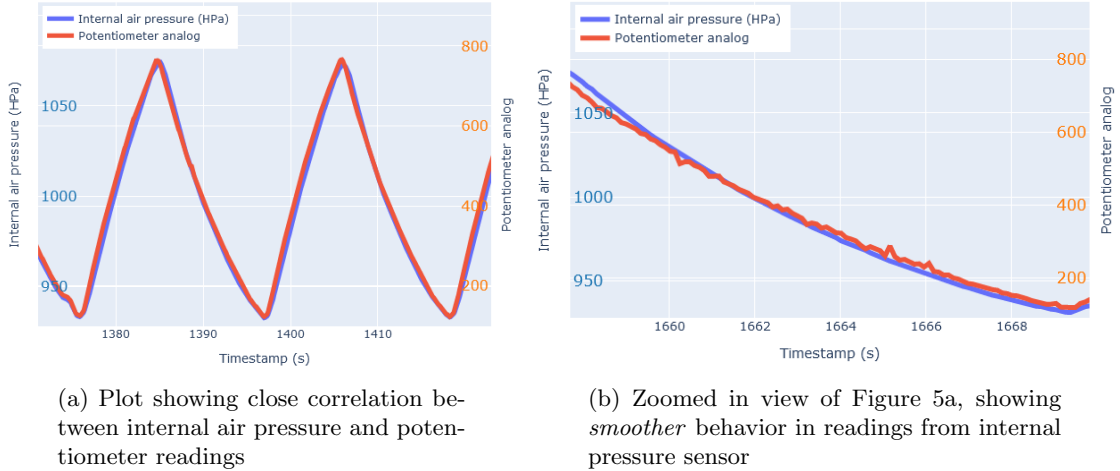


Figure 5: Plots of internal air pressure against potentiometer readings for expansion.

The measured pressure corresponds fairly well to the readings from the potentiometer, telling us that they are essentially equally correlated to the absolute expansion of the robot.

When examining Figure 5b, it can be observed that the internal air pressure exhibits a smoother curve, compared to the potentiometer readings. This smoothness is attributed to the increased resolution achieved by utilizing the air pressure as a measurement of expansion. The MS5611 pressure sensor, used to monitor internal pressure, offers a pressure reading resolution down to  $0.012\text{hPa}$  [11]. In the specific example, the internal pressure spans a range of  $147.7\text{hPa}$ , resulting in a total of 12,308 effective steps within this range. Thus the resolution of the pressure sensor is approximately 18.5 times greater than the 665 steps provided by the potentiometer within the same expansion range. However, the pressure sensor will have fewer effective steps, when operating in lower pressure environments, because its resolution is fixed to an absolute change in pressure. I.e.  $0.012\text{hPa}$  over a  $200\text{hPa}$  range provides 20 times as many steps as  $0.012\text{hPa}$  over a  $10\text{hPa}$  range.

## 5.5 Additional Findings in Buoyancy Control

During experimentation, some additional qualitative discoveries were made regarding the expansion mechanism and buoyancy control.

### 5.5.1 Calculated Density As Measurement Of Buoyancy

Previous experiments have used the potentiometer values as measures of buoyancy, because using density requires additional calculations on top of the raw measurements, and can be prone to errors. These calculations require knowing the total volume or weight of the robot as it was during each experiment, as well as knowing the point at which the robot has a density of  $1 \text{ kg/L}$ . Approximating these values by measuring the volume of the prototype, we have plotted the absolute external pressure against the approximated density in Figure 6. Change in density is calculated by the current expansion of the robot.

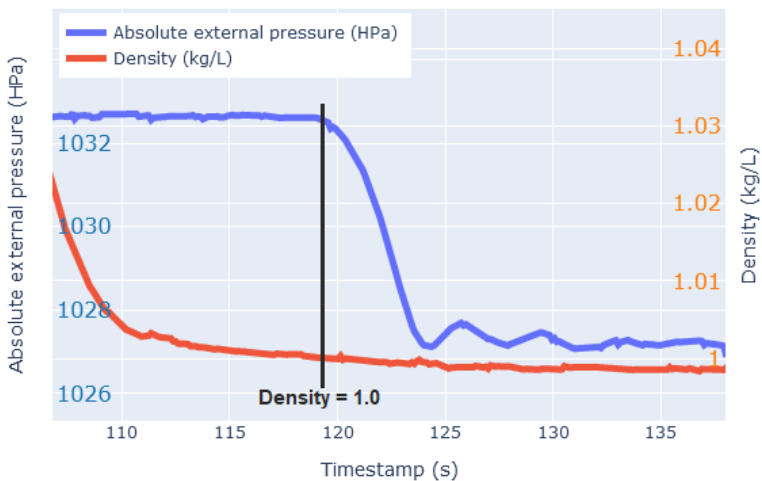


Figure 6: Plot of approximated density against external liquid pressure.

The plot shows the absolute pressure dropping as the approximated density crosses below 1, which means the robot begins rising through water. This indicates that the density approximation is close to what we expect the density to be at each point.

### 5.5.2 Momentum Creating Bobbing Motion

When the robot moves through an interface, it exhibits a bobbing motion due to its momentum, which causes fluctuations in measurements following each change in buoyancy. These fluctuations are visible in Figure 7, where after each change, the robot moves to a different depth, and takes some time to stabilize.

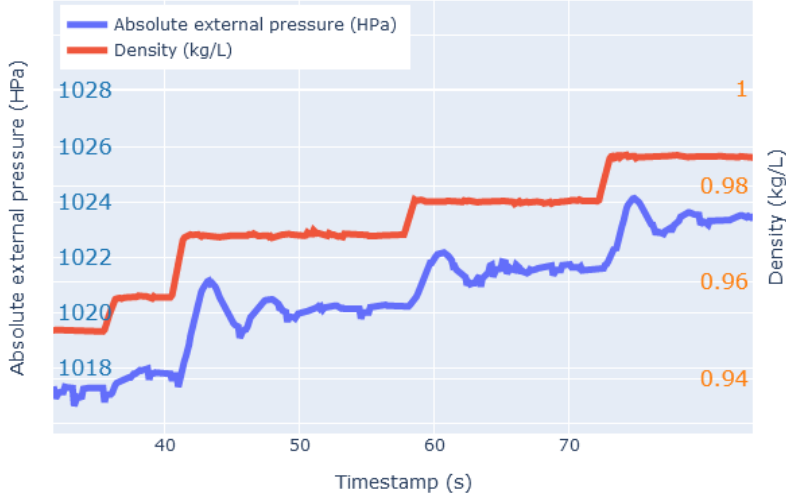


Figure 7: Plot of absolute external pressure exhibiting bobbing motion after each change in buoyancy.

As the robot moves through the interface, it does not fall straight through, but instead places itself partly between each liquid. Whenever the robot's density is set to a value between the densities of the two liquids, it will stay at a point inside the interface, where the mix of the two liquids' density would equal the density of the robot. This is why the graph exhibits a stair-stepping effect, as the robot sinks through the interface.

## 6 Discussion

During the process of building, experimenting and analyzing the results from the prototype, as well as when conducting general domain analysis, we came across several significant details and discussion points related to the respective hypotheses outlined in section 4.

### 6.1 Weight Balancing to Reduce Tilt

The prototype currently has a requirement of being balanced in an upright position. This is to keep the sensors vertically aligned. Because the linear actuator inside the robot moves the internals back and forth, the robot's centre of gravity will shift, especially if the robot is horizontally oriented.

Even when the robot is positioned upright, slight tilt can still occur, which should be minimized in order for the differential pressure sensor data to be reliable, as even slight deviations in angle can impact the calculations, as seen in section 5.3. The robot is featured with a manual weight balancing system, with small protruding rods for placing counterweights on, in order to manipulate the centre of gravity. This is however only a solution to balance the overall centre of gravity, in order to counteract any off-balancing that stems from the construction.

Because the robot's centre of gravity will always be slightly offset from the actual center of the robot, perfect balancing is difficult to achieve. Slight imperfections in balancing the robot's internals would put off the centre of gravity, and would be amplified during operation as the internals shift.

### 6.2 Tilt Compensation

Due to the design of the prototype, it is necessary for the robot to maintain a vertical orientation, as the probes of the differential pressure sensor are fixed vertically 3cm apart. Any tilt on the robot would currently impair its ability to determine the density of liquids.

The results presented in section 5.3 show a clear correlation between the angle of the probes and pressure data, as long as the distance between the probes remain at a constant distance. We do however see some "lag" in the data, meaning that after some time, the readings stabilize to the predicted point, which hinders the responsiveness of the robot slightly. However, this is also in an experiment with human intervention, distinct steps, and very exaggerated angles, rather than natural gradual tilt. It would have been valuable to also test slight gradual tilt, as it would be closer to what the robot experiences during operation.

A complete understanding of the differential pressure sensor's response to various angles would make it possible to develop a corrective function for pressure readings, albeit at the expense of some accuracy, due to the density being calculated from a lower depth difference. This approach makes it possible to determine whether a change in density is due to a change in liquid or tilt on the robot.

In order to capture the tilt angle of the robot, the onboard GY-86 IMU sensor can be used. The sensor can capture the forces acting on the robot, the angular velocity, and its orientation. It features an accelerometer, gyroscope and magnetometer, and by combining their data, it is possible to capture fairly stable and accurate measurements which makes it possible to construct a complete three dimensional view of the robot's current orientation. The IMU features an MPU6050 accelerometer [7], which can use the gravity force vector to capture the current roll (rotation about the X-axis) and pitch (rotation about the Y-axis) for the robot, but not the yaw (rotation about the Z-axis), as the force vector of gravity does not change during the rotation [8].

To capture the yaw, we can look to the HMC5883L magnetometer. The magnetometer acts as a digital compass, and can provide accuracy of within 1-2 degrees [6]. Combining the data above with the MPU6050 gyroscope, which cannot capture absolute values, but rather sense rotation in all the axes, fairly stable results can be acquired. For even better results, by using some kind of filter on the data, such as a low pass filter or Kalman Filter, the final result can be fairly accurate while maintaining relatively low noise [17].

By capturing a complete model of the robot's current orientation, in combination with sampling from the readings of the angled differential pressure sensor, it would be possible to create a density estimation algorithm, that does not rely on the robot having a low, centred, centre of gravity, as any form of tilt could be compensated for, completely automatically.

While tilt compensation can support pressure readings as the angle of tilt increases, the difference in pressure reported by the sensor can still shrink to a point where compensation cannot make the readings sufficiently precise anymore.

### 6.3 Measuring Depth with IMU VS Absolute Pressure Sensor

The robot uses pressure sensors to measure external pressure. This, in turn, necessitates having tubing running from the inside to the outside. Additionally, it requires knowledge of the density of the current liquid, which also introduces additional tubing. These tubes are potential points of failure for the robot in terms of waterproofing integrity, as they are a direct channel between the liquid and electronics. This could make alternative depth measuring systems more attractive.

There are other ways of measuring depth, such as optical and ultrasonic sensors, but they have certain limitations, such as the need for clear visibility, correct orientation, and extra infrastructure. An alternative approach that can overcome these challenges is to utilize an IMU to estimate depth. An IMU is a device that can measure a body's current forces, angular velocity and orientation. It can be used as a positional tracking device using these measurements.

The IMU could simplify the external housing as it would simply monitor the forces applied to the robot from inside the housing itself, whereas pressure sensors require a connection to the outside environment. It provides a more straightforward approach to measuring depth by capturing direct movement, while a pressure sensor requires more complex depth calculations involving liquid density.

Using this method, the robot can be placed at a known starting depth as a reference point. Then, from this point, it is possible to use subsequent acceleration and orientation measurements to calculate changes in position, as the robot moves through the liquid. By integrating acceleration data over time, velocity can be determined, and by integrating velocity over time, the position of the robot can be determined relative to the initial reference point. In this way, it is possible to roughly estimate the relative depth of the robot.

The main issue with using an IMU, is that it uses inertia, which makes all captured data relative to previous measurements, resulting in errors compounding over time.

Since our prototype uses an absolute pressure sensor to measure depth, the measured value is absolute and always in reference to the pressure in a vacuum [16]. This removes the danger of faulty readings or compound error impacting the data.

Both approaches are entirely possible, however the prototype uses the pressure based approach, to avoid the compounding error of the IMU.

## 6.4 Buoyancy Control

The prototype has specific requirements in order to accurately regulate its buoyancy. It is necessary that it can deliver enough force for expansion, it has to monitor its current level of expansion, and be able to calculate its current buoyancy at any given time.

We discovered some issues that the prototype had in relation to these requirements, such as potentiometer readings being affected by mechanical issues, cavities filling with liquids, and excessive force required to operate the expansion mechanism.

### 6.4.1 Alternative Method of Monitoring Robot Expansion

Monitoring the expansion of the robot through the linear potentiometer turned out to have mechanical issues, such as play in the construction, which in turn reduces precision and overall resolution. We investigated the possibility of using the internal pressure as a substitute to solve this issue.

Using internal pressure has the added benefit of being very versatile, as the sensor simply needs to be within the internal chamber to measure expansion. Due to Boyle's law, knowing the volume of air at any point during expansion, will enable the calculation of any volume by only the pressure reading. Potentiometers or encoders require knowledge of how much a given movement of a motor equates to a given volume change.

As seen in section 5.4, there is a very clear correlation between the robot's physical expansion, and its internal air pressure. This means that there is no need for having a linear potentiometer in the robot, as long as there is an internal pressure sensor.

Having an internal pressure sensor also allows for detecting any breach in water/air tightness, as any unexpected pressure change would be due to an integral fault during operation, such as an air containment breach.

### 6.4.2 Cavities In Robot Housing Trapping Liquids Through Phases

The current prototype design has cavities in both the top and the bottom, as it is designed as a tube with movable rubber gaskets inside, with hollow end-stops at each end.

These cavities are recessed below the surface in such a way that a cup is formed, in both the top and bottom. When the robot moves up or down through an interface, the liquid from the previous phase will be stuck in these cavities. The liquid cannot escape, due to it either being heavier or lighter than the surrounding liquid, as well as surface tension holding on to the liquid.

This trapped liquid can alter the buoyancy of the robot, as there is now unaccounted for liquids stuck in the cavities, slightly lifting up or weighing down the robot, throwing off the density calculations somewhat.

The issue of cavities is inherent to the design, and a horizontally oriented robot would not have this issue.

### 6.4.3 Overcoming Expansion Force Limitations

While conducting the experiments, we experienced some difficulty with expanding or contracting the mechanism in certain situations. One way of mitigating this issue is to adjust the pressurization of the robot before submersion. At greater depths, the hydrostatic pressure will heavily compress the robot, so to aid the mechanism in expanding in deep environments, high initial pressurization can support the mechanism, although making operation at shallow depth more difficult. Friction in the system is likely another factor which contributes to issues with movement. The movable gaskets are always in contact with the walls, so one way to address this might be to use more or different lubricants to ensure smooth movement.

There is also the possibility that the gaskets might become misaligned with each other or the housing walls. This misalignment could create a significant amount of additional friction. Misalignment can be caused by uneven distribution of external pressure or uneven lubrication. It is also possible that the movement of the gaskets unevenly rubs away the lubrication due to imperfections in the assembly. These misalignment issues could be addressed by including stabilizers for the gaskets or by stiffening the entire assembly to reduce slack.

## 6.5 Further Work

Having explored the challenges and complexities in underwater buoyancy-manipulating robots, it is important to consider potential avenues for future research and development. The primary objective of this investigation was to design and implement an underwater buoyancy-manipulating robot, capable of precise buoyancy control, to locate interfaces in multi-phase liquids. By reviewing and analyzing the current design and prototype, we have identified areas for further work and attention that will enhance and expand the capabilities of the robot.

### 6.5.1 Mapping a Column of Multiple Liquids

Locating interfaces might in some cases require finding depths of more than one liquid interface. While we have not explored locating multiple interfaces through experiments, there are ways for a moving robot to use differential pressure to theoretically map the locations of all interfaces in a liquid column.

The ability to do this is, however, dependent on the assumption that the robot can already reliably determine the correct density and depth of the liquid it is submerged in, and possesses reliable movement in the liquid.

Multi-phase mapping can be done in two ways, depending on whether the phases are taller than the height of the robot or not.

#### Assuming Phases Are Taller Than Robot

In the case that each liquid phase is taller than the height of the robot, the robot can be in motion without operating the mechanism, while sinking or rising through a continuous phase. Using the absolute pressure sensor to detect this type of motion, the location of the interface can be determined as the point where the robot stops sinking by itself.

When the robot is moving through an interface, it will stay at a certain depth somewhere in between the liquids, depending on its own density in relation to the density of the two liquids of the interface. Using small changes in buoyancy, the robot can be compressed until it is all the way through an interface, and sinks through the phase to the next interface on its own. The previous steps are repeated, until the entire column of liquid is mapped.

## Assuming Interfaces Might Be Shorter Than Robot

In the case that interfaces might be shorter than the robot's height, we cannot rely on detecting motion without altering buoyancy, as the robot might always be in between liquids.

This problem is solved by inferring the unknown density of the liquid below the interface, from the known density of the one above the interface, and the ratio of each liquid, as measured by the robot.

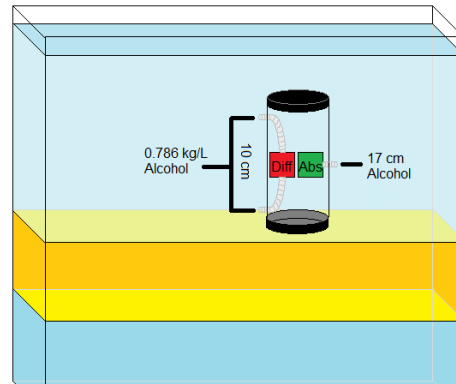
When locating interfaces in this manner, it is required to know the density of the very top liquid, for example by it being taller than the robot, or by taking a sample.

To explain the principle through an example with mapping interfaces in water, sunflower oil and rubbing alcohol:

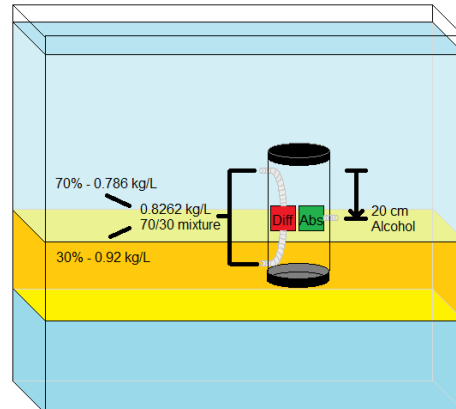
The differential pressure probes on the robot are 10 cm apart, and the absolute pressure probe is between the two, with 5 cm to each. The robot is in the top phase, measuring a density of  $0.786 \text{ kg/L}$ , which is the density of rubbing alcohol (shown in Figure 8a). Knowing the density means that the depth can be mapped in the entirety of this phase by the absolute pressure.

When compressing the robot, the measured density begins to increase, as it passes through the first interface, but the depth can still be measured by the old density until the absolute pressure probe reaches the interface 5 cm down (Figure 8b). This means that before the absolute pressure sensor passes through the interface, we know the exact volumetric proportions between the liquids, based on the absolute depth the robot has sunk. 3 cm through the interface, the density is measured at  $0.8262 \text{ kg/L}$ . Knowing that 70% (7 cm) of the mixture has a density of  $0.768 \text{ kg/L}$ , the remaining 30% has to have the density  $0.92 \text{ kg/L}$ , which is the density of sunflower oil.

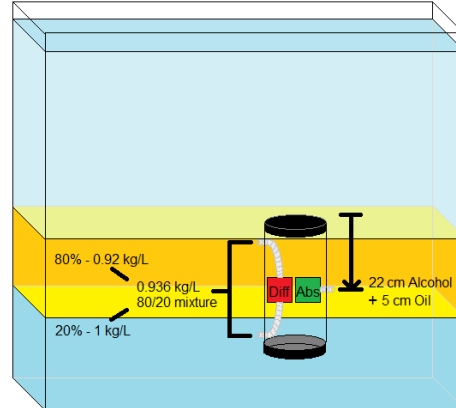
From this point, we can predict the changes in density until the robot is through the interface, and if readings diverge from the prediction, we will know it has discovered the oil/water interface. The same method can then be applied to that interface as well (see Figure 8c).



(a)



(b)



(c)

Figure 8: Diagram of robot and density calculations when traveling through rubbing alcohol, sunflower oil and water

### **6.5.2 Characterizing Emulsion In Liquids**

One big question is how would it be possible to tackle two different liquids, which does not have a clear interface between them, but rather a layer of emulsion separating them. The interface is no longer a fine line, but instead a gradient spanning over a variable distance. This can cause issues due to the way that the prototype currently finds interfaces.

This phenomenon is very common in the application of finding interfaces between crude oil and water, where crude oil often contains a lot of contaminants that settle in emulsion layers between the oil and water [5].

Currently, we find interfaces by adjusting the robot's buoyancy until it settles on top of an interface, but in the case of an emulsified interface, there is no clear top or bottom, and finding the beginning of the gradient requires infinitely precise sensors. However, the robot will still find a buoyant equilibrium point somewhere into the emulsion layer, where it stays still.

Using the theory described in section 6.5.1 for finding multiple interfaces, an emulsion can be described as many, very small, phases on top of each other. Each phase can then be seen as having its own density, increasing throughout the emulsion.

We theorize that it is difficult to work with emulsified interfaces, but have not characterized the behavior of the robot in an emulsified liquid, apart from this theory. To create accurate models of the behavior, physical experiments will likely have to be carried out.

### **6.5.3 Alternative Methods of Volume Change**

The prototype we have built, changes its volume by one-dimensional expansion with a linear actuator. This has caused issues with balancing the centre of gravity and intended orientation.

By using the gathered knowledge that internal air pressure can tell the expansion of any shape or mechanism, the robot does not need to be constrained to one-dimensional expansion. If it is possible to create a robot with uniform expansion in all three dimensions, problems such as centre of gravity and orientation could be disregarded.

## 7 Conclusion

In conclusion, this paper has described a successful proof of concept for an interface-locating, buoyancy regulating robot. The robot successfully addresses the challenges associated with controlling its volume and buoyancy in multi-phase liquid environments. By incorporating features such as electromechanical actuation, continuous monitoring of total expansion, and precise buoyancy estimation, the robot demonstrates high potential for various applications.

The robot uses a measurement of its current volume to calculate its density and buoyancy. It can make precise adjustments to its total volume to reach a desired density, which lets it efficiently navigate diverse liquid environments. The robot captures pressure data to determine the depth of liquid interfaces, by matching the density of different liquids. The measured effectiveness of the robot's depth sensing is:

- Resolution of depth measurements:  $0.135\text{cm}$  in water, extrapolated from pressure resolution of  $0.1323\text{hPa}$ .
- Relative and absolute accuracy of oil/water interface location within 6.8% and  $0.73\text{cm}$  respectively.

The measured effectiveness of the robot's density sensing is:

- Precision of density measurements in oil of  $0.00597\text{kg/L}$ .
- Precision of density measurements in water of  $0.01251\text{kg/L}$ .
- Relative and absolute accuracy of density measurements in oil of  $\pm 1.4\%$  and  $\pm 0.0127\text{kg/L}$  respectively.<sup>1</sup>
- Relative and absolute accuracy of density measurements in water of  $\pm 1.4\%$  and  $\pm 0.014\text{kg/L}$  respectively.<sup>1</sup>

The measured effectiveness of the robot's expansion mechanism is:

- A total volume change of  $102.64\text{ ml}$ .
- 890 effective steps over 3 cm, when using potentiometer attached to actuator. Resolution of  $0.115\text{ ml}$  volumetric expansion per step.
- Accuracy of  $1.1\%FS$  when using potentiometer attached to actuator.
- 12,308 effective steps in example, when measuring expansion through internal air pressure. Resolution down to  $0.012\text{hPa}$  over a  $147.7\text{hPa}$  range.

We have discovered some requirements that have to be met for a functioning prototype of this kind of autonomous robot. When using differential pressure sensors, the probes have to be vertically aligned, or the tilt on the alignment has to be compensated for, because the density calculations rely on a known depth between the probes. Additionally, robots in this domain should always have a measurement of their own buoyancy, taking external influences into account. This becomes a problem for our prototype when it travels through interfaces, as it can collect liquid from each phase in cavities in its shape. Finally, the required force for the actuator has to be predetermined as strong enough to counteract external forces such as air pressure, hydrostatic pressure or friction. They raise the force requirements and can make operation at certain depths difficult.

---

<sup>1</sup>Accuracy calculated from averaged values, because outliers make single-value accuracy calculations impractical.

Moving forward, further refinements and improvements can be made to enhance the robot's performance and expand its capabilities. Examples for further work include an in-depth implementation of our presented algorithm for mapping a column of multiple liquids, further understanding and characterization of emulsion in liquids, as well as exploring alternative methods of volume change.

## 8 References

- [1] Peter A. Ciullo and Norman Hewitt. "Physical testing of rubber". In: *The Rubber Formulary* (1999), pp. 55–72. DOI: 10.1016/b978-081551434-3.50005-1.
- [2] Syed Bukhari and Wuqiang Yang. "Multi-interface Level Sensors and New Development in Monitoring and Control of Oil Separators". en. In: *Sensors* 6.4 (Apr. 2006), pp. 380–389. ISSN: 1424-8220. DOI: 10.3390/s60400380. URL: <http://www.mdpi.com/1424-8220/6/4/380> (visited on 02/03/2023).
- [3] Clifford A. Pickover. *Archimedes to hawking: Laws of science and the great minds behind them*. Oxford University Press, 2008.
- [4] Irina Nita. "Study of the behavior of some vegetable oils during the thermal treatment". In: *Analele Universitatis Ovidius Constanta* 21 (Jan. 2010), p. 5. URL: [http://anale-chimie.univ-ovidius.ro/anale-chimie/chemistry/2010-1/full/1\\_nita.pdf](http://anale-chimie.univ-ovidius.ro/anale-chimie/chemistry/2010-1/full/1_nita.pdf).
- [5] Mahmoud Meribout, Ahmed Al, and Khamis Al. "Interface Layers Detection in Oil Field Tanks: A Critical Review". en. In: *Expert Systems for Human, Materials and Automation*. Ed. by Petric Vizureanu. InTech, Oct. 2011. ISBN: 978-953-307-334-7. DOI: 10.5772/17166. URL: <http://www.intechopen.com/books/expert-systems-for-human-materials-and-automation/interface-layers-detection-in-oil-field-tanks-a-critical-review> (visited on 01/29/2022).
- [6] 3-Axis Digital Compass IC HMC5883L. Rev. E. Honeywell. Feb. 2013. URL: [https://cdn-shop.adafruit.com/datasheets/HMC5883L\\_3-Axis\\_Digital\\_Compass\\_IC.pdf](https://cdn-shop.adafruit.com/datasheets/HMC5883L_3-Axis_Digital_Compass_IC.pdf).
- [7] MPU-6000 and MPU-6050 Product Specification. PS-MPU-6000A-00. Revision 3.4. InvenSense Inc. Aug. 2013. URL: <https://invensense.tdk.com/wp-content/uploads/2015/02/MPU-6000-Datasheet1.pdf>.
- [8] Tilt Sensing Using a Three-Axis Accelerometer. AN3461. Rev. 6. NXP Freescale Semiconductor. Mar. 2013. URL: <https://www.nxp.com/docs/en/application-note/AN3461.pdf>.
- [9] Jules Jaffe et al. "A swarm of autonomous miniature underwater robot drifters for exploring submesoscale ocean dynamics". In: *Nature Communications* 8 (Jan. 2017), p. 14189. DOI: 10.1038/ncomms14189.
- [10] Bangyuan Liu et al. "Electromechanical Control and Stability Analysis of a Soft Swim-Bladder Robot Driven by Dielectric Elastomer". In: *Journal of Applied Mechanics* 84.9 (July 2017). 091005. ISSN: 0021-8936. DOI: 10.1115/1.4037147. eprint: <https://asmedigitalcollection.asme.org/appliedmechanics/article-pdf/84/9/091005/6084840/jam\_084\_09\_091005.pdf>. URL: <https://doi.org/10.1115/1.4037147>.
- [11] MS5611-01BA03 Barometric Pressure Sensor, with stainless steel cap. MS5611-01BA03. TE Connectivity. June 2017. URL: [https://www.te.com/commerce/DocumentDelivery/DDEController?Action=showdoc&DocId=Data+Sheet%7FMS5611-01BA03%7FB3%7Fpdf%7FEnglish%7FENG\\_DS\\_MS5611-01BA03\\_B3.pdf%7FCAT-BLPS0036](https://www.te.com/commerce/DocumentDelivery/DDEController?Action=showdoc&DocId=Data+Sheet%7FMS5611-01BA03%7FB3%7Fpdf%7FEnglish%7FENG_DS_MS5611-01BA03_B3.pdf%7FCAT-BLPS0036).

- [12] Robert Katzschmann et al. “Exploration of underwater life with an acoustically controlled soft robotic fish”. In: *Science Robotics* 3 (Mar. 2018), eaar3449. DOI: 10.1126/scirobotics.aar3449.
- [13] Arnaldo G. Leal-Junior et al. “Multi-interface level in oil tanks and applications of optical fiber sensors”. In: *Optical Fiber Technology* 40 (2018), pp. 82–92. DOI: 10.1016/j.yofte.2017.11.006.
- [14] Mads Ørnfeldt Wolf Jespersen (mads\_1997@live.dk) Julian Brandt (contact@julianbrandt.dk) Nicolai Pallund (nicolai@pallund.dk). “Research on underwater robots with variable buoyancy”. In: (Dec. 2022).
- [15] Dingeman L.H. van der Haven et al. “Parameterless detection of liquid–liquid interfaces with sub-micron resolution in single-molecule localization microscopy”. In: *Journal of Colloid and Interface Science* 620 (2022), pp. 356–364. ISSN: 0021-9797. DOI: <https://doi.org/10.1016/j.jcis.2022.03.116>. URL: <https://www.sciencedirect.com/science/article/pii/S0021979722005112>.
- [16] Avnet Abacus. *Absolute pressure sensors*. URL: <https://www.avnet.com/wps/portal/abacus/solutions/technologies/sensors/pressure-sensors/measurement-types/absolute/> (visited on 05/23/2023).
- [17] Alex Becker. *Kalman Filter*. URL: <https://www.kalmanfilter.net/default.aspx> (visited on 05/23/2023).

# Appendices

## A Prototype model and dimensions

During the course of the project, we made or imported models of all components to aid in the design of the robot. An image of an assembly of all models can be found in figure 9.

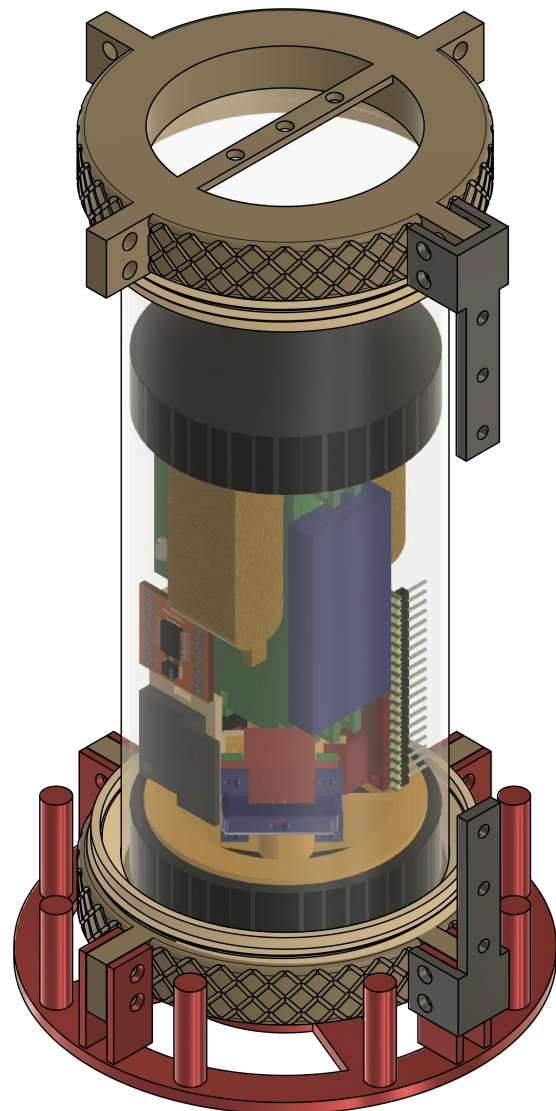


Figure 9: Modeled assembly of prototype

## B Prototype Technical Drawing

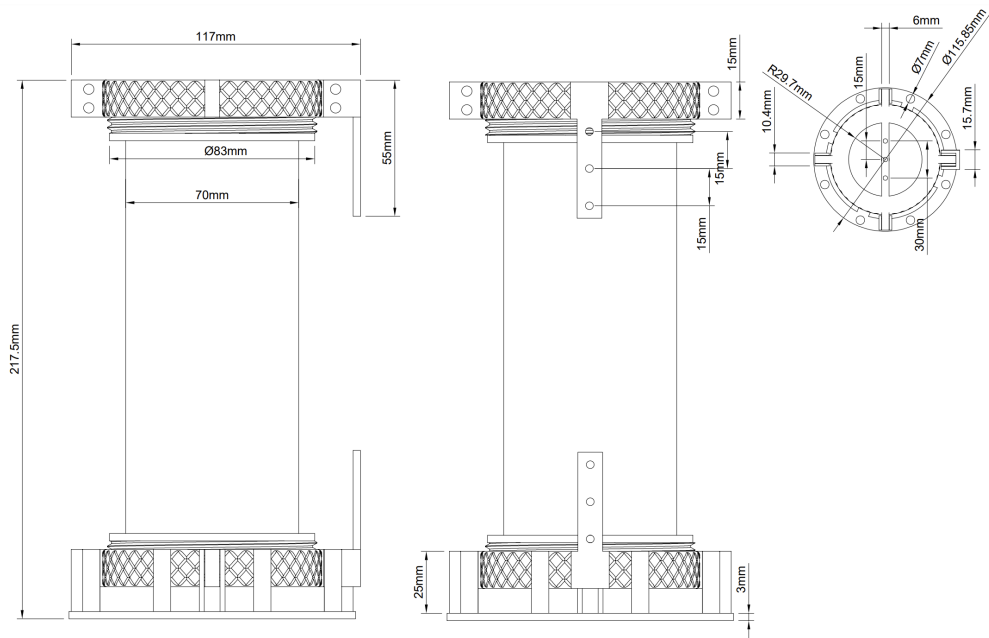


Figure 10: Drawing of prototype with dimensions

## C Prototype Wiring Diagram

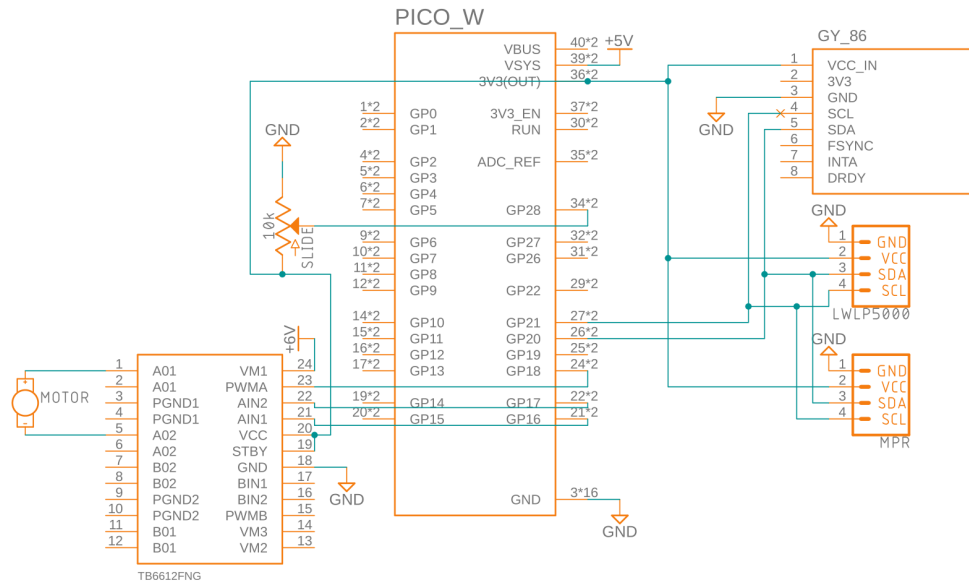


Figure 11: Wiring diagram of the prototype

## D Photograph of Prototype in Oil/Water Interface

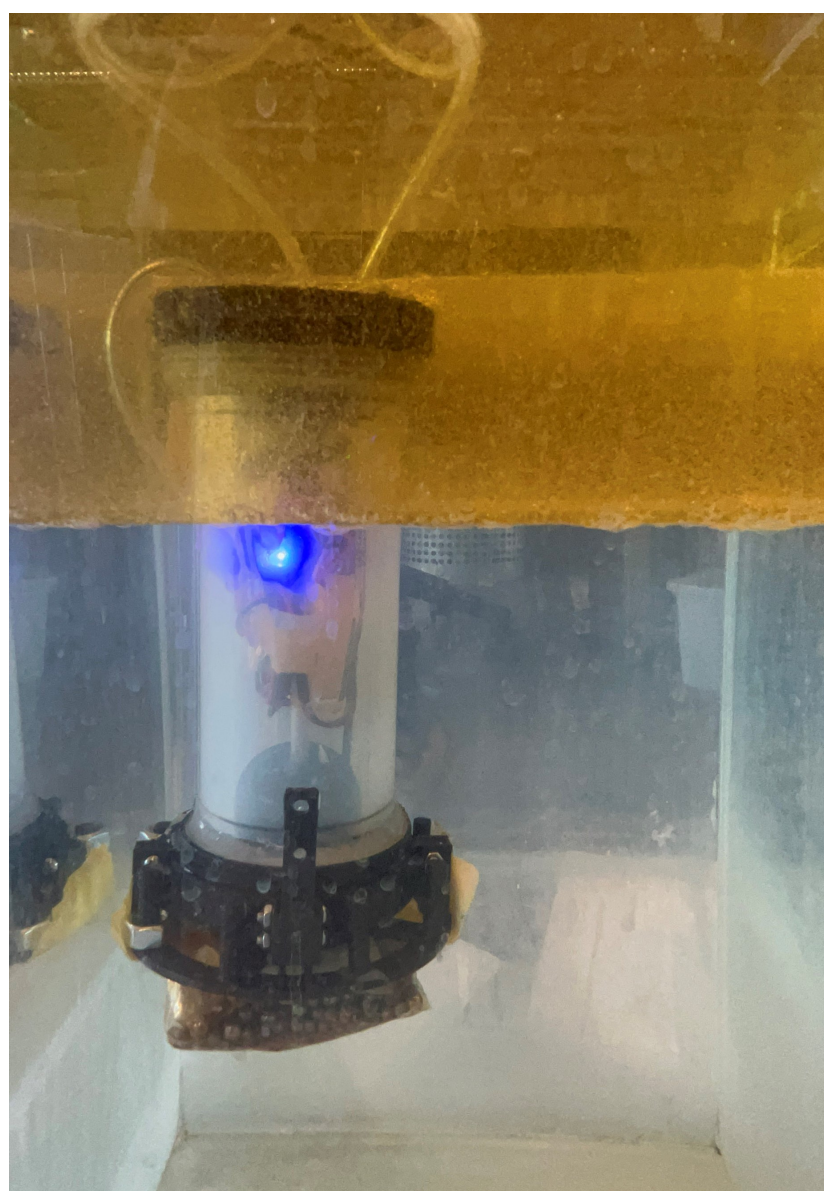


Figure 12: Prototype in the middle of an interface between water and sunflower oil.

## E Relevant 3D Printed Parts



(a) Jig used to keep the two ends of the differential pressure sensor probes 3 cm apart while rotating during experiments.



(b) Spacing jig used to keep the two ends of the differential pressure sensor probes 3cm apart during experiments.



(c) Jig used to place the spacing jig onto. The two levels are for the two different liquids and is used to move between the liquids consistently.

Figure 13: Relevant 3D parts and jigs used for experiments.